Biological Chemistry ‘Just Accepted’ Papers

Biological Chemistry ‘Just Accepted’ Papers are papers published online, in advance of appearing in the print journal. They have been peer-reviewed, accepted and are online published in manuscript form, but have not been copy edited, typeset, or proofread. Copy editing may lead to small differences between the Just Accepted version and the final version. There may also be differences in the quality of the graphics. When papers do appear in print, they will be removed from this feature and grouped with other papers in an issue.

Biol Chem ‘Just Accepted’ Papers are citable; the online publication date is indicated on the Table of Contents page, and the article’s Digital Object Identifier (DOI), a unique identifier for intellectual property in the digital environment (e.g., 10.1515/hsz-2011-xxxx), is shown at the top margin of the title page. Once an article is published as **Biol Chem ‘Just Accepted’ Paper** (and before it is published in its final form), it should be cited in other articles by indicating author list, title and DOI.

After a paper is published in **Biol Chem ‘Just Accepted’ Paper** form, it proceeds through the normal production process, which includes copy editing, typesetting and proofreading. The edited paper is then published in its final form in a regular print and online issue of **Biol Chem.** At this time, the **Biol Chem ‘Just Accepted’ Paper** version is replaced on the journal Web site by the final version of the paper with the same DOI as the **Biol Chem ‘Just Accepted’ Paper version.**

Disclaimer

Biol Chem ‘Just Accepted’ Papers have undergone the complete peer-review process. However, none of the additional editorial preparation, which includes copy editing, typesetting and proofreading, has been performed. Therefore, there may be errors in articles published as **Biol Chem ‘Just Accepted’ Papers** that will be corrected in the final print and online version of the Journal. Any use of these articles is subject to the explicit understanding that the papers have not yet gone through the full quality control process prior to advanced publication.

Biological Chemistry 'Just Accepted' paper
ISSN (online) 1437-4315
DOI: 10.1515/hsz-2018-0342

Research Article

An engineered lipocalin that tightly complexes the plant poison colchicine for use as antidote as well as bioanalytical applications

Mikhail Barkovskiy, Elena Ilyukhina, Martin Dauner, Andreas Eichinger and Arne Skerra*

Munich Center for integrated Protein Science (CiPSM) and Lehrstuhl für Biologische Chemie, Technische Universität München, 85354 Freising (Weihenstephan), Germany

*Corresponding author

e-mail: skerra@tum.de

Abstract

Colchicine is a toxic alkaloid prevalent in autumn crocus (*Colchicum autumnale*) that binds to tubulin and inhibits polymerization of microtubules. Using combinatorial and rational protein design, we have developed an artificial binding protein based on the human lipocalin 2 that binds colchicine with a dissociation constant of 120 pM, i.e. 10 000-fold stronger than tubulin. Crystallographic analysis of the engineered lipocalin, dubbed Colchicalin, revealed major structural changes in the flexible loop region that forms the ligand pocket at one end of the eight-stranded β-barrel, resulting in a lid-like structure over the deeply buried colchicine. A *cis*-peptide bond between residues Phe71 and Pro72 in loop #2 constitutes a peculiar feature and allows intimate contact with the tricyclic ligand. Using directed evolution, we achieved an extraordinary dissociation half-life of more than 9 h for the Colchicalin•colchicine complex. Together with the chemical robustness of colchicine and availability of activated derivatives, this also opens applications as a general-purpose affinity reagent, including facile quantification of colchicine in biological samples. Given that engineered lipocalins, also known as Anticalin® proteins, represent a class of clinically validated biopharmaceuticals, Colchicalin may offer a therapeutic antidote to scavenge colchicine and reverse its poisoning effect in situations of acute intoxication.

Keywords: Anticalin; Colchicalin; directed evolution; intoxication; lipocalin 2; protein engineering.

Introduction

Colchicine (**1**, Figure 1A) is an alkaloid found in diverse species of the *Liliaceae* family, in particular autumn crocus (*Colchicum autumnale*) and glory lily (*Gloriosa superba*). Colchicine acts by binding to tubulin, the major protein component of microtubules, thereby altering the association/dissociation kinetics of microtubule monomers and favoring depolymerization (Banerjee & Luduena, 1987; Panda *et al.*, 1995). This leads to inhibition of several crucial cellular functions such as formation of the mitotic spindle apparatus, cellular motility and intracellular trafficking (Kreutzberg, 1969; Malawista, 1968). However, if applied in small doses, colchicine exerts an anti-inflammatory effect and, therefore, has been in use as a drug for treatment of acute gout flares for centuries (Hartung, 1954). Today, colchicine is also applied to treat familial Mediterranean fever, Behçet's syndrome, and other inflammatory diseases (Cerquaglia *et al.*, 2005; Niel & Scherrmann, 2006; Miyachi *et al.*, 1981).

The inhibitory effect of colchicine on neutrophil motility and activity likely explains the beneficial pharmacological properties of this drug, whereas its systemic toxicity at higher doses can be attributed to the antimitotic activity on dividing cells, in particular in intestinal epithelium and bone marrow, as well as to the disruption of axonal transport (Malawista, 1968; Nuki, 2008). In fact, colchicine intoxication results in gastrointestinal damage, aplastic anemia and disseminated intravascular coagulation, followed by multiple organ failure. In fatal cases, cardiac arrest and sudden asystole typically occur before the development of other hematological complications, hence representing the most common cause of death in human patients (Folpini & Furfori, 1995; Klintschar *et al.*, 1999; Stapczynski *et al.*, 1981; Borron *et al.*, 1996; Brvar *et al.*, 2004).

Colchicine intoxications are known to happen accidentally as well as intentionally. Accidental poisoning often results from confusion of autumn crocus with bear's garlic (*Allium ursinum*), an edible plant used in national cuisines of Central Europe (Klintschar *et al.*, 1999; Danel *et al.*, 2001; Brncić *et al.*, 2001; Brvar *et al.*, 2004). Both plants occupy similar biotopes and are difficult to distinguish outside the blooming season, which can lead to ingestion of *Colchicum* in amounts sufficient for lethal intoxication. On the other hand, in cases of suicide or even murder, the toxin is usually derived from colchicine-based drugs which are sold prescription-free in many countries (Danel *et al.*, 2001; Nagesh *et al.*, 2011; Deveaux *et al.*, 2004; Link *et al.*, 2014).

Unfortunately, treatment of colchicine overdose is difficult: after ingestion, the small molecule (399 Da) is quickly absorbed into tissues (terminal distribution volume in humans: 6.7 l/kg) while its concentration in blood drops within 1–2 h down to the nanomolar range (Rochdi *et al.*, 1994; Wallace & Ertel, 1970); this pharmacokinetic behavior prevents efficient removal by hemodialysis. Although supportive therapy increases the chances of recovery (Link *et al.*, 2014), the treatment remains symptomatic, and clinical statistics reveal that digestion of more than 0.8 mg colchicine per kg body weight almost always is lethal (Stapczynski *et al.*, 1981).

Colchicine-specific antibodies and/or Fab fragments derived from immunized goat (Sabouraud *et al.*, 1991; Terrien *et al.*, 1990) or sheep (Eddleston *et al.*, 2018; Peake *et al.*, 2015) have been successfully used to reverse colchicine toxicity *in vitro* in cell culture, *in vivo* in mice and pigs and, anecdotally, in one human patient (Terrien *et al.*, 1990; Sabouraud *et al.*, 1991; Baud *et al.*, 1995; Peake *et al.*, 2015; Eddleston *et al.*, 2018). One drawback of immunoglobulin-based antidotes is their high molecular mass, which necessitates injection of large quantities of protein to achieve stoichiometric neutralization of the toxin (Baud *et al.*, 1995). As another caveat, all antibody-based antidotes against colchicine reported so far comprise polyclonal sera derived from animals (Sabouraud *et al.*, 1991; Baud *et al.*, 1995; Peake *et al.*, 2015), thus lacking defined composition and posing a high risk of immunogenicity.

To develop a novel antidote against colchicine, we employed Anticalin® technology (Gebauer & Skerra, 2012; Richter *et al.*, 2014; Rothe & Skerra, 2018) employing the small and robust protein scaffold of the human lipocalin 2 (Lcn2, also known as neutrophil gelatinase-associated lipocalin, NGAL, or as siderocalin), which naturally scavenges bacterial siderophores as part of the innate immune system (Goetz *et al.*, 2002; Correnti & Strong, 2012; Dauner *et al.*, 2018). All members of the lipocalin family share a β-barrel fold formed by eight antiparallel β-strands that form a ligand pocket at the open end (Schiefner & Skerra, 2015; Skerra, 2000). For antidote applications, such engineered lipocalins offer several advantages over antibodies and their fragments: (i) they offer a deep ligand pocket, which is well suited for tight binding of small molecules (haptens); (ii) they lack immunological effector functions and are not recognized by receptors or removed from the blood stream by specific cellular uptake; (iii) their constitution as small and robust single-chain proteins facilitates high-yield production in bacterial host cells.

In a previous example, an Anticalin based on the bilin-binding protein (BBP) from the butterfly *Pieris brassicae* was developed against the cardioactive plant steroid digoxigenin (Schlehuber *et al.*, 2000) and successfully used to reverse digitalis intoxication in guinea pig and rat models (Schlehuber & Skerra, 2005; Eyer *et al.*, 2012). In the present study, we have employed human Lcn2 as a scaffold for the directed evolution of a colchicine-specific binding protein suitable both as antidote and for bioanalytical applications.

Results

Selection of a lipocalin specific for colchicine from a random library

To make colchicine amenable as a molecular target for selection and to enable its immobilization on the surface of streptavidin-coated paramagnetic beads, we attached a D-biotin moiety via a PEG_3-Abu linker to the free amino group of colchicine after deacetylation (Figures 1 and S1). For selection via phagemid display, an Lcn2 random library with a combinatorial complexity of $1x10^{10}$ was employed (Gebauer *et al.*, 2013). After two cycles of phagemid panning on colchicine-charged magnetic beads, the mutated lipocalin gene cassette was prepared as a pool and subcloned on a vector for bacterial surface display (Binder *et al.*, 2010; Gebauer & Skerra, 2012) followed by fluorescence-activated cell sorting (FACS) using biotinyl-colchicine (**2**) and a streptavidin-phycoerythrine (PE) conjugate (Figure 1B). After six FACS cycles, the population converged to a single lipocalin variant, which was dubbed D6.1. Its affinity towards biotinyl-colchicine (**2**) was initially assessed via FACS titration of a cultured single clone (Figure 1C, D). Curve fit of the mean fluorescence intensity (MFI) versus ligand concentration revealed an apparent affinity of approximately 7 nM. In the next step, this lipocalin candidate was expressed and purified as a soluble monomeric protein and its affinity towards free (acetylated) colchicine (**1**) was measured via fluorescence titration, resulting in a K_D of 3.6 ± 0.1 nM (see below).

Affinity improvement of the selected colchicine-specific lipocalin

To further boost its binding activity, we subjected D6.1 to an affinity maturation procedure. To this end, the central part of the gene cassette, which encodes the four structurally variable loops of the lipocalin, was moderately mutagenized using an error-prone polymerase chain reaction (PCR), thus yielding a gene library comprising $2x10^9$ variants with an average

mutation rate of approximately 3 amino acids per gene. As it is impractical to screen more than 10^8 cells using FACS technology, we introduced a pre-enrichment step using magnetic cell selection (MACS) as recently described (Friedrich *et al.*, 2017).

In this procedure, *E. coli* cells displaying the mutated lipocalin were incubated with streptavidin-coated paramagnetic beads charged with biotinyl-colchicine (**2**). After intensive washing, those bacteria that remained bound to the beads were amplified in culture medium. The population with reduced complexity resulting from this single enrichment step was further subjected to FACS. To achieve more stringent selection compared with the initial FACS of the naïve library, we (i) decreased the ligand (**2**) concentration from 10 µM to 10 nM, (ii) shortened the incubation time with the ligand to 1 min and (iii) introduced a competitive dissociation step; to this end, the bacteria were additionally incubated with an up to 1000-fold excess of free colchicine (**1**) in order to prevent re-association of the biotinylated ligand (**2**).

In the third FACS cycle, the error-prone lipocalin library showed a strong signal even after competitive dissociation overnight, whereas almost no binding was detectable for the initial clone D6.1 when subjected to the same assay conditions as an individual culture (Figure 2A, B). After the fifth cycle, we analyzed 48 clones for binding activity via FACS by applying 4 nM biotinyl-colchicine (**2**) and, thereafter, analyzed the 12 best clones by DNA sequencing. All 12 sequences were unique but shared a pattern of three conserved amino acid substitutions: V69M, I80T, and F83L (Figure 2C).

To individually investigate the role of each mutation, we introduced these amino acid exchanges into the original clone D6.1 using site-directed mutagenesis, one-by-one and in different combinations. The resulting lipocalin variants were produced as soluble proteins in *E. coli* (Figure 3) and their affinities towards free colchicine were measured by fluorescence titration (Table 1) of a 100 nM protein solution. Of all tested variants, the triple mutant V69M/I80T/F83L showed the highest affinity, in the pM range, and this colchicine-binding lipocalin variant – from now on, Colchicalin – was designated D6.2. For more precise assessment, fluorescence titration of D6.2 was also performed using a 20 nM protein solution, which provided better resolution of the binding curve and led to a K_D value of 120 pM (Figure 4).

During the mutational analysis, the substitution Val69Met appeared to be most crucial, as this side chain exchange alone led to a 10-fold increase in ligand affinity compared with D6.1 (Table 1). However, as surface-exposed Met side chains are prone to oxidation (Walsh, 2007), we tried replacing this position with a different residue having a β-unbranched side chain. Interestingly, substitution of Met with Ala and Leu resulted in about 5-fold reduction of affinity whereas substitution with Gln maintained the high affinity of D6.2 and even showed an additional benefit: a two-fold increase in expression yield. Consequently, the mutant D6.2(M69Q) was used for crystallographic analysis.

X-ray crystallographic analysis of the Colchicalin•colchicine complex

Initial attempts to crystallize the engineered lipocalin in its full-length format, including an affinity tag (*Strep*-tag II or His_6-tag), remained unsuccessful. Consequently, we minimized the N- and C-terminal flexible regions in D6.2(M69Q) by both removing the affinity tag and deleting the 4 N-terminal amino acids, which often remained unresolved in previous crystal structures of other engineered lipocalins. To this end, we constructed a fusion protein carrying an N-terminal SUMO domain with a His_6-tag, which was expressed in the less reducing cytoplasm of *E. coli* Origami B, purified by immobilized metal ion affinity chromatography (IMAC) and cleaved with Ulp1 protease (Malakhov *et al.*, 2004). The tag-free lipocalin protein was isolated by subtractive IMAC and size exclusion chromatography (SEC).

After complex formation with a slight excess of colchicine, the resulting variant Δ4-D6.2 (M69Q) was crystallized in the presence of 2.2 M $(NH_4)_2SO_4$, 200 mM Li_2SO_4 and 100 mM Tris/HCl pH 7.5. The crystal structure with space group $P4_122$ at a resolution of 2.2 Å (Table S1) was solved by molecular replacement. The refined structural model (Figure 5) comprised residues Ser5–Gly178 as well as bound colchicine with well-defined electron density and the expected stereochemistry. Residues Ile97–Pro101, corresponding to the variable loop #3 of the engineered lipocalin, showed weaker density as reflected by elevated B-factors.

The structural analysis revealed high shape complementarity between the engineered lipocalin and the small ligand colchicine, which resulted from a major rearrangement of the flexible loop region at the open end of the β-barrel. On the other hand, the lipocalin fold overall remained virtually identical to the wild type Lcn2 structure (Goetz *et al.*, 2002) with a root mean square deviation (RMSD) of 0.83 Å for 58 structurally conserved Cα positions

(Skerra, 2000). The higher RMSD of 2.51 Å that was calculated when comparing all 172 structurally defined Cα positions is a consequence of the structural deviations seen for loop #2 (bent inward by up to 11.1 Å), loop #3 (bent inward by up to 6.4 Å) and loop #4 (bent outward by up to 7.3 Å), whereas the conformation of loop #1 remained essentially conserved – despite its extended length (Figure 5A).

Loops #2 and #3 form a narrow, cleft-like entrance to the deep binding pocket, which buries the tricyclic colchicine ligand. In contrast, enterobactin, the natural ligand of Lcn2, is bound in a rather shallow pocket and partly exposed to the solvent. As expected from the use of the biotinylated target compound for selection, the acetyl substituent of colchicine appears accessible at the entrance of the ligand pocket, whereas the three annealed rings of colchicine are densely packed among multiple aromatic amino acid side chains: Phe41, Phe68, Phe71, Trp106, Phe123 and Phe134. Of note, only Phe71 and Phe123 correspond to the wild-type lipocalin, whereas the other residues were introduced during the combinatorial design process.

A PISA analysis revealed that 88.7% of the total solvent-accessible surface area of colchicine (547.7 of 617.7 $Å^2$) becomes buried upon complexation (Table S2, Figure 5D). The phenyl groups of residues Phe41, Phe123 and Phe134 form a peculiar aromatic cluster. Phe68 is involved in a π-stacking interaction with the aromatic ring A of colchicine. Phe71 interacts with one side of the tropone ring C while Trp106 covers a large part of its opposite side. Apart from two glycine residues, 7 hydrophilic amino acids contact the ligand. Three of these constitute Thr residues (Thr54, Thr104 and Thr 136) whereas four are charged: Lys70, Asp81, Arg130, Asp132 (cf. Table S2); however, the side chains of Lys70 and Asp81 point away from colchicine.

The most striking feature of the engineered lipocalin structure is the conformation of loop #2, which is shifted towards the ligand by up to 11.1 Å (at the Cα position of residue Phe71); this allows the Phe side chain to stack against the colchicine ring C, thus shielding most of its hydrophobic surface from solvent. Moreover, the backbone nitrogen of Phe71 forms a hydrogen bond with the acetamide group of colchicine. The unusual conformation of loop #2 is accompanied by a *cis*-peptide bond with the following residue Pro72 (a randomized position), which constitutes a rare feature in the engineered lipocalins that have been structurally investigated up to now. Interestingly, loop #2 also encompasses the position Gln69 (or Met69 in the variant D6.2), the most important mutation selected during the affinity maturation as explained above.

Another notable feature of the complex between Colchicalin and colchicine is the presence of 3 water molecules at the very bottom of the ligand pocket, which are engaged in a network of 10 hydrogen bonds. 7 hydrogen bonds anchor the water molecules in the protein cavity (via OH-groups of Thr54 and Tyr138, backbone oxygen of Ala52 as well as backbone nitrogen and oxygen of Gln69) while 3 hydrogen bonds link them to the oxygen atoms of two methoxy substituents of colchicine ring A. The position of Tyr138 is further stabilized by a hydrogen bond with Tyr56. Involvement of residue Gln69 in this extended hydrogen bonding network – replacing Val in wild type Lcn2 or Met in D6.2 – may explain its beneficial effect on the binding activity as described above.

Fine-tuning of affinity towards colchicine

The ligand affinity of the engineered lipocalin D6.2 is already in the range of available polyclonal antibody fragments directed against colchicine (Peake *et al.*, 2015; Baud *et al.*, 1995) and, thus, should be sufficient for *in vivo* application as an antidote. Beyond that, the relatively long half-life of the Colchicalin•colchicine complex of 1.5 h (see Figure 4C) prompted the idea of using Colchicalin as an immobilization reagent, similar to the well-established systems based on D-biotin, fluorescein or digoxigenin (Wilchek *et al.*, 2006; Voss, 1984; McCreery, 1997). To this end, an even longer complex half-life would be desirable.

To further improve the stability of the ligand complex, the engineered lipocalin D6.2 (carrying the Met69 residue) was subjected to an additional cycle of affinity maturation involving error-prone PCR and FACS in combination with bacterial surface display; this time, the selection pressure was even more increased to favor slow dissociation kinetics by applying a 10 000-fold excess of free colchicine in the competition step and incubating the bacteria for 16 h at a higher temperature of 8 °C (instead of 0 °C). After 5 FACS cycles, 3 mutant lipocalins were isolated, sequenced and, after preparation as soluble proteins, tested for colchicine-binding activity via real-time surface plasmon resonance (SPR) spectroscopy.

For these measurements, a colchicine derivative carrying a short PEG linker with a free amino group (colchicine-PEG-amine, **8**) was synthesized and covalently coupled to the sensor chip (Figure S1, bottom). Two of the three tested variants, EI.1 and EI.3 (Figure 2C), showed dissociation half-lives of more than 3 h (Table S3). Since both variants exhibited unique sets of amino acid substitutions, we recombined them by individually introducing the three

additional mutations found for EI.1 into EI.3, which was chosen as acceptor because of its better expression yield and slightly lower k_{off} value. Each point mutant was produced as a soluble protein, purified and again tested by SPR. One of these mutations, K142I, decreased the dissociation rate of EI.3 by almost 2-fold, yielding the lipocalin variant D6.4 with a dissociation half-life of 5.3 h.

Moreover, based on the crystal structure of D6.2(M69Q) in complex with colchicine described above, the hydrophilic Thr136 residue, which is situated in a local hydrophobic environment in direct proximity to the ligand, was substituted by Val providing a more hydrophobic side chain of similar size. This side chain exchange in D6.4 resulted in the variant D6.5 with a further increased dissociation half-life of 6.7 h. Finally, we introduced the mutation Gln77Glu, which was observed several times during the earlier affinity maturation of the variant D6.1 (not shown), thus yielding the Colchicalin D6.6. This variant had a particularly low k_{off} value of $2x10^{-5}$ s^{-1} and a remarkable complex half-life of 9.4 h (Figure 4C).

Development of a competitive ELISA for sensitive detection of colchicine in biological samples

Up to now, quantification of colchicine in diagnostic samples depends on high end LC-MS analytics (Abe *et al.*, 2006; Fabresse *et al.*, 2017). To enable fast diagnosis of colchicine intoxication in body fluids, we developed a simple competitive ELISA (Figure 6A) with sensitivity down to the single-digit nanomolar range utilizing the Colchicalin D6.2 (Figure 6B). In this setup, the bottom of a microtiter plate well is directly coated with the engineered lipocalin whereas biotinyl-colchicine **2** serves as competitive tracer. After optimizing the concentrations of D6.2 and tracer, we were able to detect and quantify colchicine in concentrations down to 1 nM. Presence of 1% v/v human serum in the analyte solution did not affect the sensitivity of the assay (see Figure S2). Our novel immunochemical method enables quantification of colchicine in plain serum using cheap equipment and without laborious sample preparation (such as extraction of colchicine with organic solvents as required for HPLC analytics).

Discussion

We have described the selection of a lipocalin that binds colchicine with sub-nanomolar affinity, thus providing a promising antidote for treatment of acute colchicine poisoning. We have also demonstrated the possibility of using this lipocalin as a reagent for colchicine quantification and as a tool for *in vitro* biomolecular immobilization. In the past years, Lcn2-based Anticalin proteins were developed against various disease-related target molecules, including proteins (CTLA4 and the ED-B domain of fibronectin) (Schönfeld *et al.*, 2009; Gebauer *et al.*, 2013), peptides (Aβ) (Rauth *et al.*, 2016) and hapten-type ligands such as Fe^{III}•petrobactin (Dauner *et al.*, 2018) or Y^{III}•DTPA (Kim *et al.*, 2009), both resembling the natural siderophore ligands of Lcn2 (Abergel *et al.*, 2008; Goetz *et al.*, 2002). In the present study, we were able to demonstrate that Anticalin® technology also allows the facile selection of high-affinity binding proteins towards a fully unrelated low molecular weight compound such as colchicine.

X-ray structural analysis of the engineered lipocalin in complex with this ligand revealed that the combination of amino acid exchanges provided for by the lipocalin random library design, with a few additional substitutions acquired during affinity maturation, led to structural rearrangements that would have been difficult to predict. The resulting Colchicalin D6.2 constitutes a high-affinity binding protein that surpasses the binding activity of natural lipocalins. For example, the crucial residue Phe71 remained unchanged from the wild type Lcn2 scaffold but is brought into close contact with the bound colchicine due to a major conformational rearrangement of the flexible loop #2. Both the newly introduced *cis*-Pro residue at the following position, which appeared early during the combinatorial selection process, and the substitution Val69 to Met/Gln had a remarkable effect on the orientation of loop #2. As a consequence, this loop forms a lid-like structure over the ligand pocket, exemplifying an unprecedented structural mechanism that might be useful for the development of engineered lipocalins against other small molecules in the future.

The combination of phagemid display and bacterial surface display of the lipocalin variants in a functional state was another crucial factor for the success of this endeavor. Use of phage display in the early stage of selection allowed us to sample a much higher library complexity ($>1x10^{10}$) than possible by FACS alone. On the other hand, bacterial surface display provided better control over selection at the later stages and simplified the preliminary screening of promising candidates via single-clone analysis prior to subcloning and functional analysis of

the purified proteins. As we were interested in the structure-function relationships of the lipocalin variants that emerged in the course of selection, we also investigated the effects of individual mutations on their binding properties. This allowed us to keep the number of functionally irrelevant mutations, which normally accompany sequence randomization, at minimum, thus reducing the risk of immunogenicity of the human lipocalin scaffold upon future therapeutic application.

Colchicine poisoning – both occasional and suicidal – remains a persistent problem in clinical toxicology, both due to the time-consuming analytics and the lack of effective therapeutic options. Although, in principle, the application of Fab fragments against colchicine was shown to reverse colchicine intoxication in one human patient (Baud *et al.*, 1995), no specific anti-colchicine antidote has reached market approval to date. This may in part be explained by the fact that such intoxications happen rarely and do not easily justify the costly development of a suitable drug by a pharmaceutical company. However, simplification and international harmonization of procedures that regulate approval of treatments for rare diseases ('orphan drugs') might alleviate this situation. Notably, Anticalin® technology has reached clinical stage for several drug candidates and proven safety and efficacy in early studies (Rothe & Skerra, 2018). In fact, engineered human lipocalins offer several advantages over antibodies, such as cheaper production and a lower molecular mass, which both favor the stoichiometry of colchicine complexation and tissue penetration. Based on previous *in vivo* studies with an Anticalin that neutralizes the digitalis toxin (Eyer *et al.*, 2012), our new Colchicalins appear promising for the effective scavenging of poisonous colchicine from blood and tissues in an acute therapeutic setting.

Furthermore, the Colchicalin-based ELISA developed here should facilitate the fast and simple diagnosis of colchicine poisoning, which is essential for the timely start of treatment. In clinical toxicology, colchicine is quantified in blood or urine samples using high performance liquid chromatography coupled to mass spectrometry (HPLC-MS) (Abe *et al.*, 2006; Wehner *et al.*, 2006). This time-consuming procedure requires costly analytical instrumentation that is not accessible in each hospital whereas ELISA is a routine method available in most laboratory facilities. According to clinical data, plasma concentration of colchicine within the first 24 h after intoxication lies in the range of 10–50 ng/ml (or 25–125 nM); thus, the sensitivity of our novel assay allows quantification of colchicine at toxicologically relevant concentrations. Furthermore, this ELISA may even be useful to routinely screen plant raw material for colchicine contamination in the food industry.

In conclusion, the picomolar affinities of the selected Colchicalins confirm the versatility of the Lcn2 scaffold for developing binding proteins against hapten-type ligands in general. Phylogenetic studies indicate that the lipocalin family evolved at the beginning of the eukaryote era as a family of binding proteins for small molecules (Ganfornina *et al.*, 2000). This function is enabled by their tulip-like architecture with a deep and narrow binding pocket, contrasting with the mostly shallow antigen-binding sites of antibodies. The high kinetic stability of the complex between D6.6 and colchicine also suggests that this Colchicalin can be utilized as an innovative reagent for the *in vitro* immobilization of colchicine-conjugated (bio-)molecules, thus complementing established systems based on (strept)avidin/biotin or digoxigenin- and fluorescein-binding antibodies or their fragments (Wilchek *et al.*, 2006; Voss, 1984; McCreery, 1997).

The remarkable dissociation half-life of over 9 h should be ideal for many applications, including ELISA, immunoblotting, cell staining, real-time SPR and the like, while the small size of the engineered lipocalin and its inherently monomeric structure offer practical advantages over streptavidin-, avidin- or antibody-based systems. On the other hand, colchicine is a chemically stable molecule, which can be selectively modified at its amino group after deacetylation, as demonstrated here, opening the route to commonly employed activated ester or electrophile derivates for the labelling of Lys or Cys side chains. Most importantly in this context, our X-ray analysis has revealed that the amino substituent of the colchicine tricycle points outward the binding pocket and is accessible for attachment, ideally via a linker, to other molecules without sterical interference. Toxicity of colchicine should be of little concern at the low concentration range used for most *in vitro* studies. Taken together, our Colchicalins should prove useful for diverse *in vivo* and *in vitro* applications.

Materials and methods

Chemical synthesis of biotinyl-colchicine (2)

N-Deacetylcolchicine (**5**) was prepared from colchicine (**1**) as described (Bagnato *et al.*, 2004) (Figure S1) and obtained as trifluoroacetate salt after purification by silica chromatography (eluent: dichloromethane/methanol 9:1). This salt (29 mg, 61 µmol) was dissolved, together with 18-biotinamino-17-oxo-4,7,10,13-tetraoxa-16-azaeicosan-1-oic acid succinimidyl ester (**6**, 37 mg, 55 µmol; Iris Biotech, Marktredwitz, Germany; mixture of two diastereomers) and

triethylamine (14 µl, 100 µmol), in 2 ml dry dichloromethane and stirred for 24 h at room temperature. The solvent was evaporated, and the crude product was purified by silica chromatography (eluent: dichloromethane/methanol 9:1 to 7:1). The deacetylcolchicine-PEG_3-Abu-biotin conjugate **2** was obtained as a yellow solid (42 mg, 46 µmol, 84%).

^{1}H NMR (500 MHz, Chloroform-d) δ 12.09 (br, 2 H, NH), 8.04 – 7.98 (m, 1 H, NH colch.), 7.58 (d, *J* = 2.4 Hz, 1 H, CH tropone), 7.31 (dd, *J* = 10.7, 2.5 Hz, 1 H, CH tropone), 7.16 – 7.12 (m, 1 H, NH Abu), 6.84 (dd, *J* = 11.1, 1.6 Hz, 1 H, CH tropone), 6.53 (s, 1 H, CH aromat.), 4.65 (dd, *J* = 11.8, 7.0 Hz, 1 H, CHNH colch.), 4.56 – 4.53 (m, 1 H, SCH_2CH), 4.43 – 4.39 (m, 1 H, CH Abu), 4.38 – 4.36 (m, 1 H, SCHCH), 3.98 (s, 3 H, OCH_3), 3.93 (s, 3 H, OCH_3), 3.90 (s, 3 H, OCH_3), 3.76 – 3.59 (m, 13 H, 5x CH_2 linker, OCH_3 tropone), 3.58 – 3.55 (m, 4 H, 2x CH_2 linker), 3.50 – 3.41 (m, 4 H, 2x CH_2 linker), 3.17 – 3.12 (m, 1 H, SCH), 2.94 – 2.90 (m, 1 H, SCH_2), 2.79 – 2.75 (m, 1 H, SCH_2), 2.55 (t, *J* = 6.3 Hz, 2 H, $C(O)CH_2$ linker), 2.53 – 2.49 (m, 1 H, CH_2 colch.), 2.41 – 2.34 (m, 1 H, CH_2 colch.), 2.27 (t, *J* = 7.1 Hz, 2 H, $C(O)CH_2$ biotin), 2.24 – 2.16 (m, 2 H, CH_2 colch.), 1.96 – 1.88 (m, 1 H, CH_2 colch.), 1.87 – 1.78 (m, 1 H, CH_2 Abu), 1.77 – 1.57 (m, 5 H, CH_2 Abu, 2x CH_2 biotin), 1.48 – 1.40 (m, 2 H, CH_2 biotin), 0.94 – 0.84 (m, 3 H, CH_3 Abu).

^{13}C NMR (126 MHz, Chloroform-d) δ 179.41 & 179.39 (C(O)), 173.44 & 173.40 (C(O)), 172.6 & 172.4 (C(O)), 171.14 & 171.10 (C(O)), 164.1 (m, C(O), COMe tropone), 153.6, 152.3, 151.3, 141.7, 137.1, 135.4, 134.5, 131.3, 125.9, 112.8, 107.6 (11x CH aromat.), 70.7 – 70.3 (m), 69.9 (m), 67.5, 67.4 (CH_2 linker), 62.1 & 62.0 (SCHCH), 61.7 ($COCH_3$ tropone), 61.5 ($COCH_3$ colch.), 60.56 & 60.55 (SCH_2CH), 56.5 ($COCH_3$ colch.), 56.3 ($COCH_3$ colch.), 55.6 & 55.4 (SCH), 54.60 & 54.56 (CH Abu), 52.1 (CHNH colch.), 40.7 & 40.5 (SCH_2), 39.51 & 39.48 ($NHCH_2$ linker), 36.9 – 36.8 (m, CH_2 linker, CH_2 colch.), 35.7 & 35.5 ($C(O)CH_2$ biotin), 30.2 (CH_2 colch.), 28.1 & 28.0 (CH_2), 27.9 & 27.8 (CH_2), 26.2 & 26.0 (CH_2), 25.61 & 25.56 (CH Abu), 10.2 & 10.1 (CH_3 Abu).

HR-ESI-MS: calc. $[M + H]^+$ = 916.4373, $[M – H]^-$ = 914.4226; found $[M + H]^+$ = 916.4358, $[M – H]^-$ = 914.4219

Chemical synthesis of colchicine-PEG-amine (8)

21-(Boc-amino)-4,7,10,13,16,19-hexaoxaheneicosanoic acid (**7**, 52.9 mg, 117 µmol; Sigma-Aldrich, Munich, Germany), 4-methylmorpholine (12.8 mg, 127 µmol, 14 µl) and PyBOP (66.1 mg, 127 µmol, Iris Biotech) were dissolved in 3 ml dry DMF and stirred for 30 min at

room temperature (Figure S1). Then, *N*-deacetylcolchicine trifluoroacetate (**5**) from above (50 mg, 106 µmol) was added as a solid, and the mixture was stirred for another 16 h at room temperature. The solvent was removed under vacuum, 4 ml dichloromethane/trifluoroacetic acid (1:1) was added, and the mixture was stirred for 30 min at room temperature to cleave the Boc protecting group, followed by solvent removal under vacuum. After purification by HPLC on a Nucleodur C18 Gravity column (5 µm, 250x10 mm; Macherey Nagel, Düren, Germany) using a gradient of 27–30% v/v acetonitrile in 0.1% w/v aqueous TFA over 10 min (flow rate 3 ml/min; t_R = 7 min), the resulting colchicine-PEG-amine **8** was obtained as a yellow oil (31.3 mg, 45 µmol, 43%).

^{1}H NMR (400 MHz, Methanol-d4) δ 7.43 – 7.38 (m, 2 H, aromat.), 7.24 – 7.18 (m, 1 H, aromat.), 6.78 – 6.73 (m, 1 H, aromat.), 4.54 – 4.47 (m, 1 H, C<u>H</u>NH), 4.01 (s, 3 H, OCH_3), 3.90 (s, 3 H, OCH_3), 3.88 (s, 3 H, OCH_3), 3.75 – 3.55 (m, 28 H, 2x OCH_3, 11x OCH_2), 3.08 (t, *J* = 5.2 Hz, 2 H, $NH_2C\underline{H}_2CH_2O$), 2.70 – 2.55 (m, 2 H, CH_2), 2.54 – 2.44 (m, 1 H, CH_2), 2.36 (td, *J* = 13.1, 6.9 Hz, 1 H, CH_2), 2.30 – 2.14 (m, 1 H, CH_2), 1.95 (td, *J* = 12.2, 6.8 Hz, 1 H, CH_2).

^{13}C NMR (101 MHz, MeOD) δ 180.8, 173.5, 165.4, 155.2, 154.0, 152.2, 142.7, 138.5, 137.6, 136.0, 131.5, 126.8, 114.9, 108.7, 71.4 – 70.7 (m, OCH_2), 68.2, 67.9 ($C(O)CH_2\underline{C}H_2$, $\underline{C}H_2CH_2NH_2$), 61.9 (OCH_3), 61.6 (OCH_3), 57.0 (OCH_3), 56.7 (OCH_3), 53.7 (CHNH), 40.5 (CH_2NH_2), 37.4 ($C(O)\underline{C}H_2$), 37.3 (CH_2 tropone), 30.5 (CH_2 tropone).

HR-ESI-MS: calc. $[M + H]^+$ = 693.35930, $[M + 2\ H]^{2+}$ = 347.18329; found $[M + H]^+$ = 693.37568, $[M + 2\ H]^{2+}$ = 347.22861

Phage display of the naïve lipocalin random library

For phage display selection, a naïve lipocalin random library comprising $1x10^{10}$ variants cloned on the phagemid vector pNGAL108 was used (Gebauer *et al.*, 2013), which carries the mutated Lcn2 gene fused with the bacterial OmpA signal sequence and the pIII minor coat protein of the filamentous phage M13. Phagemid selection was performed according to a published procedure (Gebauer & Skerra, 2012). Briefly, biotinyl-colchicine **2** from above (Figure 1A) was immobilized on streptavidin- or NeutrAvidin-coated paramagnetic beads (Sigma-Aldrich or Thermo Fisher Scientific, Waltham, MA, respectively), which were blocked with 2% w/v bovine serum albumin (BSA; Sigma-Aldrich) in phosphate-buffered saline (PBS) containing 0.1% v/v Tween-20 (PBS/T). The beads were incubated with the

phagemid library (starting titer $1x10^{12}$) in a total volume of 400 µl for 1 h. After ten washing steps with PBS/T, each for one minute, bound phagemids were eluted with 400 µl of 100 µM free colchicine (AppliChem, Darmstadt, Germany) in PBS for 1.5 h. The eluted phagemids were used to infect exponentially growing *E. coli* XL1-blue cells (Stratagene, San Diego, CA); amplified phagemids were purified and subjected to the next selection cycle (in total two cycles).

Bacterial surface display of lipocalins using FACS

After enrichment of colchicine-specific lipocalin variants by phagemid display, pooled phasmid DNA was prepared, and the variable gene cassette was excised via the pair of flanking *Bst*XI restriction sites and subcloned on the vector pNGAL146 for bacterial surface display (Gebauer & Skerra, 2012). To this end, a fusion protein comprising the mutant lipocalin equipped with the OmpA signal peptide, an A3C5 peptide tag and the engineered β-domain of the bacterial autotransporter EspP was employed (Binder *et al.*, 2010). Electrocompetent *E. coli* K-12 JK321 (Jose *et al.*, 1996) cells were transformed with the ligation mixture and plated onto LB agar containing 100 mg/l ampicillin to yield $1.7x10^8$ transformants. The bacteria were scraped from the agar plates, resuspended in 50 ml Luria Bertani (LB) medium containing 100 mg/l ampicillin and used to inoculate 200 ml of LB/Amp medium to a starting OD_{550} = 0.2. The culture was incubated under shaking at 30°C until OD_{550} = 0.5 was reached, then protein expression was induced by adding 10 ng/ml anhydrotetracycline (ACROS Organics, Geel, Belgium). After 2.5 h, a 200 µl aliquot of the culture (approximately $2x10^8$ cells) was spun down, washed once by resuspending in 1 ml PBS and incubated with a mixture of 10 µM biotinyl-colchicine **2** and 3 µM anti-A3C5-Fab-DY634 conjugate (Binder *et al.*, 2010) in a total volume of 50 µl PBS for 1 h. The cells were washed again and stained with 100 nM streptavidin-phycoerythrin (PE) conjugate (BD Biosciences, Heidelberg, Germany) in 50 µl PBS for 10 min. After another washing step with PBS, the bacteria were finally centrifuged, resuspended in 1 ml PBS and used for sorting in a FACSAria instrument (BD Biosciences). In each sorting cycle, approximately 0.5% of the population with the strongest binding signal was gated. The collected bacteria were plated on LB agar supplemented with 100 mg/l ampicillin, incubated overnight at 37°C and subjected to the next sorting cycle (in total six cycles).

For affinity maturation of the variant D6.1, the incubation time with biotinyl-colchicine was reduced and an additional competition step was introduced to increase the stringency of

selection: after incubating with 10 nM biotinyl-colchicine **2** in 100 µl PBS for 1 min, the bacterial pellet was washed and incubated with 1–10 µM colchicine (**1**) in PBS containing 0.5% (w/v) BSA at 4–8°C for up to 16 h. After that, the bacteria were washed, stained with a mixture of 3 µM anti-A3C5-Fab-DY634 and 100 nM streptavidin-PE in 25 µl PBS and subjected to FACS as described above.

FACS analysis of cultured single clones was used to assess the ligand affinities of lipocalin variants. To this end, *E. coli* cells displaying the relevant variant were incubated with a dilution series of biotinyl-colchicine **2** (instead of a fixed concentration), followed by staining with streptavidin-PE as above and quantification of the mean fluorescence intensities (MFI). The dissociation constant was deduced by non-linear regression of the following formula: $MFI = MFI_{max} \times L_{tot} / (K_D + L_{tot})$.

>Generation of error-prone lipocalin libraries

The Lcn2 gene cassette flanked by the pair of *Bst*XI restriction sites, which encompasses all four structurally variable loops of the protein scaffold (Gebauer & Skerra, 2012), was mutated using the GeneMorph II Random Mutagenesis Kit (Agilent, Santa Clara, CA). 50 pg plasmid DNA were applied as template in a 50 µl polymerase chain reaction (PCR). The PCR product was purified using the Wizard SV Gel and PCR Clean-Up System (Promega, Madison, WI), digested with *Bst*XI and inserted into pNGAL146 for bacterial surface display. The resulting gene library carried approximately 3 amino acid exchanges per clone on average, as determined by DNA sequencing of sample transformants. After transformation of *E. coli* K12 JK321 as above, a library with a complexity of $2.2 \cdot 10^9$ was obtained.

Library pre-enrichment via magnetic cell selection (MACS)

E. coli JK321 cells transformed with the error-prone lipocalin library were prepared in the same manner as described above for the FACS procedure to effect surface display of the lipocalin variants. After addition of anhydrotetracycline (10 ng/ml), the bacterial culture (200 ml) was incubated for 1.5 h, then the bacteria were spun down, washed twice by resuspending in 10 ml PBS containing 0.5% (w/v) BSA and centrifuged again. The bacterial pellet was resuspended in 50 ml of 10 nM biotinyl-colchicine **2** in the same buffer and incubated for 2 h on ice. After one washing step, the bacteria were resuspended in 10 ml of the same buffer and mixed in a 15 ml tube with 1 mg streptavidin-coated paramagnetic beads (Roche Diagnostics, Mannheim, Germany), which had previously been washed three times in

the same buffer. The suspension was incubated for 1 h at 4°C on a tube roller. Then, the beads with bound bacteria were collected with a magnet, washed twice with 5 ml of the buffer, resuspended in 1 ml LB medium and plated onto LB agar containing 100 mg/l ampicillin. After incubation overnight at 37°C, the bacterial colonies were scraped from the plates and used for FACS as above.

Protein expression and purification

Lipocalin variants were produced as monomeric proteins with a C-terminal *Strep*-tag II (Schmidt & Skerra, 2007) in the periplasm of *E. coli* JM83 using the OmpA signal sequence following published procedures (Gebauer & Skerra, 2012). Cultivation was performed at 22°C in shake flasks with 2 l LB medium containing 100 mg/l ampicillin; recombinant gene expression was induced with 200 ng/ml anhydrotetracyclin at OD_{550} = 0.5. After 3 h, bacteria were harvested by centrifugation and the periplasmic proteins were extracted. The lipocalin proteins were purified via *Strep*-Tactin Superflow affinity chromatography (IBA, Göttingen, Germany) and size-exclusion chromatography (SEC) on a Superdex 75 10/300 GL column (GE Healthcare, Munich, Germany).

Protein-ligand fluorescence titration

A colchicine stock solution (40 or 8 µM) was added in 0.25–4 µl aliquots to 2 ml of a purified solution of the lipocalin (100 or 20 nM, respectively) in PBS and the decrease in Tyr and Trp fluorescence (excitation at 280 nm, emission at 345 nm) was monitored using an LS50B spectrophotometer (Perkin Elmer, Waltham, MA) equipped with a 4 ml quartz cuvette (Hellma Analytics, Müllheim, Germany) and a magnetic stirrer. Since colchicine absorbs at 345 nm, a control titration of *N*-acetyltryptophanamide was carried out to correct for the inner filter effect. Curve fitting was performed using a published equation (Vogt & Skerra, 2001) with Origin Pro software (OriginLab, Northampton, MA).

Surface plasmon resonance (SPR) spectroscopy

Colchicine-PEG-amine **8** was immobilized on a CM5 sensor chip (GE Healthcare Bio-Sciences, Uppsala, Sweden), which had been activated with 1-ethyl-3-(-3-dimethylaminopropyl)carbodiimide (EDC) and *N*-hydroxysuccinimide (NHS) according to the manufacturer's recommendations. A 1:2 dilution series of the lipocalin variant from 128 to 1 nM was prepared in PBS containing 0.005% v/v Tween-20, which also served as

running buffer. Samples were analyzed on a Biacore 2000 instrument (Biacore, Uppsala, Sweden) at 25°C using the following parameters: flow rate 25 µl/min, association for 4 min, dissociation for 100 min. For the experiment shown in Figure 4C, 100 µl of each lipocalin variant at a concentration of 256 nM was injected. The chip surface was regenerated by injecting 10 µl 0.5% w/v SDS after each run. The data were fitted according to the 1:1 Langmuir binding model with the equation $\Delta AB/\Delta t = k_{on} \times A \times B - k_{off} \times AB$, wherein k_{on} and k_{off} are the association and dissociation rate constants, respectively, using BIAevaluation Software (GE Healthcare).

Protein crystallization

The lipocalin variant D6.2(M69Q) was produced as a C-terminal fusion with the SUMO protein (Malakhov *et al.*, 2004) carrying an N-terminal His_6-tag. Expression was achieved in the cytoplasm of *E. coli* Origami B (EMD Millipore, Billerica, MA), a strain possessing a less reducing cytoplasm and allowing formation of the structural disulfide bridge present in the lipocalin. First, *E. coli* Origami B transformed with pASK-T7RBS-2 harbouring the structural gene was cultivated at 25°C overnight in shake flasks with 2 l LB medium supplemented with 100 mg/l ampicillin. Then, the temperature was lowered to 22°C, and recombinant gene expression was induced with 200 ng/ml anhydrotetracycline at OD_{550} = 0.5. After 4 h of recombinant gene expression, the bacteria were harvested by centrifugation and disrupted in a French pressure cell (SLM Aminco, Urbana, IL). The soluble extract was purified on a Ni(II)-charged HisTrap HP column (GE Healthcare) using 150 mM NaCl, 40 mM NaP_i pH 7.4 as running buffer and applying a linear concentration gradient of imidazole/HCl. The eluate was dialyzed against running buffer and the fusion protein was digested with home-made Ulp1 protease carrying a His_6-tag for 4 h at 20°C as described (Malakhov *et al.*, 2004). The mixture was then passed through a HisTrap HP column in a subtractive chromatography, and the flow-through was concentrated to 1 ml and applied to a Superdex S75 16/60 column equilibrated with 50 mM NaCl, 10 mM MES/NaOH pH 6.0. Protein purity was assessed by SDS-PAGE with Coomassie staining. The purified protein was mixed with colchicine dissolved at 100 mM in DMF at a molar ratio of 1:1.5, concentrated to 40–50 mg/ml in an Amicon Ultra-4 concentrator (MWCO 10 kDa; Millipore, Eschborn, Germany) and subjected to crystallization via the vapour diffusion technique using an in-house precipitant screen. Initial hits were identified in nanodrops (500 nl) in 96-well plates and then refined using

1.5 µl drops on silanized glass slides. Finally, crystals were obtained after two weeks in the presence of 2.2 M $(NH_4)_2SO_4$, 200 mM Li_2SO_4 and 100 mM Tris/HCl pH 7.5.

Collection and processing of X-ray diffraction data, model building and refinement

One crystal of the Colchicalin•colchicin complex with dimensions 300x150x50 μm^3 was harvested, transferred into precipitant buffer supplemented with 30% v/v glycerol and immediately frozen in liquid nitrogen. For X-ray structure solution, a single-wavelength synchrotron data set was collected at 100 K using BESSY beamline 14.3 at the Helmholtz-Zentrum Berlin, Germany (Table S1). The diffraction data were processed with MOSFLM and SCALA (CCP4, 1994). Molecular replacement was carried out with Phaser (CCP4, 1994) using the structure of the engineered human lipocalin 2 having specificity for Y^{III}-DTPA (PDB ID: 3DTQ) (Kim *et al.*, 2009) as search model. The model was built and manually adjusted with Coot (Emsley & Cowtan, 2004). Water molecules were added with ARP/wARP, and rotamers of Asn and Gln side chains were adjusted with NQ-Flipper (Weichenberger & Sippl, 2007). The protein model was refined with Refmac5 (CCP4, 1994) including model correction using the RDB_REDO server (Joosten *et al.*, 2014) and validation with PROVE (Pontius *et al.*, 1996), ERRAT (Colovos & Yeates, 1993), Verify3D (Luthy *et al.*, 1992), PROCHECK (Laskowski *et al.*, 1993), WHAT_CHECK (Hooft *et al.*, 1996) and via the MolProbity server (Chen *et al.*, 2010). Secondary structure elements were assigned using DSSP (Kabsch & Sander, 1983), and crystal packing contacts were analyzed with PISA (Krissinel & Henrick, 2007). Graphics were prepared with PyMOL (DeLano, 2002) and electrostatics was calculated using the APBS module (Baker *et al.*, 2001).

The electron density map covered all residues from Ser5 to Ile176 of the lipocalin chain. Residue Tyr115 showed outlier ϕ and φ angles in the Ramachandran plot (Table S1) – as also seen in other crystal structures of Lcn2 or its mutants (see, e.g. PDB IDs 1L6M, 3CMP, 3DTQ) – but was well defined in the electron density. One peptide bond with *cis*-configuration was unambiguously observed between residues Phe71 and Pro72 in the structurally variable loop #2. The atomic coordinates and structure factors of the refined lipocalin•colchicine complex structure have been deposited at the Protein Data Bank (PDB), Research Collaboratory for Structural Bioinformatics (Rutgers University, New Brunswick, NJ), under accession code 5NKN.

Competitive ELISA for quantification of colchicine

A MaxiSorp F microtiter plate (Nunc, Wiesbaden, Germany) was coated overnight at 4°C with 100 µl per well of the purified lipocalin variant D6.2 at 5 µg/ml in PBS. All subsequent incubation steps were performed at room temperature and with agitation at 500 rpm in a microplate shaker with 3 mm orbit size (VWR, Darmstadt, Germany). The plate was blocked with PBS/T containing 3% w/v BSA for 1 h, washed with PBS/T, and a dilution series of free colchicine in PBS supplemented with a constant concentration of biotinyl-colchicine **2** as tracer was applied. After 1 h incubation, the plate was washed with PBS/T using an ELx405 plate washer (BioTek Instruments, Bad Friedrichshall, Germany). Then, ExtrAvidin-alkaline phosphatase (AP) conjugate (Sigma-Aldrich), diluted 1:5000 in PBS, was applied. After 1 h, the plate was washed, and bound enzyme was detected by adding 100 µl of 0.5 mg/ml *p*-nitrophenylphosphate in 0.1 M Tris/HCl, 0.1 M NaCl, 5 mM $MgCl_2$, pH 8.8. The change of absorbance at 405 nm was monitored for 30 min using a Synergy 2 photometer (BioTek Instruments). For testing possible interference with the assay human serum (off-the-clot) was obtained from PAA Laboratories (Pasching, Austria; Cat. No. C02-020).

Acknowledgements

The authors wish to thank Prof. Dr. Florian Eyer for inspiring discussions and Andreas Reichert for performing ESI-MS measurements. The authors are also grateful to Dr. Manfred S. Weiss and the BESSY beamline 14.3 of the Helmholtz-Zentrum Berlin, Germany, for technical and financial support. Anticalin® is a registered trademark of Pieris Pharmaceuticals GmbH.

References

Abe, E., Lemaire-Hurtel, A.-S., Duverneuil, C., Etting, I., Guillot, E., de Mazancourt, P. and Alvarez, J.-C. (2006). A novel LC-ESI-MS-MS method for sensitive quantification of colchicine in human plasma: application to two case reports. J. Anal. Toxicol. *30,* 210-215.

Abergel, R.J., Clifton, M.C., Pizarro, J.C., Warner, J.A., Shuh, D.K., Strong, R.K. and Raymond, K.N. (2008). The siderocalin/enterobactin interaction: a link between mammalian immunity and bacterial iron transport. J. Am. Chem. Soc. *130,* 11524–11534.

Bagnato, J.D., Eilers, A.L., Horton, R.A. and Grissom, C.B. (2004). Synthesis and characterization of a cobalamin-colchicine conjugate as a novel tumor-targeted cytotoxin. J. Org. Chem. *69,* 8987–8996.

Baker, N.A., Sept, D., Joseph, S., Holst, M.J. and McCammon, J.A. (2001). Electrostatics of nanosystems: application to microtubules and the ribosome. Proc. Natl. Acad. Sci. USA *98,* 10037–10041.

Banerjee, A. and Luduena, R.F. (1987). Kinetics of association and dissociation of colchicine-tubulin complex from brain and renal tubulin Evidence for the existence of multiple isotypes of tubulin in brain with differential affinity to colchicine. FEBS Lett. *219,* 103–107.

Baud, F.J., Sabouraud, A., Vicaut, E., Taboulet, P., Lang, J., Bismuth, C., Rouzioux, J.M. and Scherrmann, J.M. (1995). Brief report: treatment of severe colchicine overdose with colchicine-specific Fab fragments. N. Engl. J. Med. *332,* 642–645.

Binder, U., Matschiner, G., Theobald, I. and Skerra, A. (2010). High-throughput sorting of an Anticalin library via EspP-mediated functional display on the *Escherichia coli* cell surface. J. Mol. Biol. *400,* 783–802.

Borron, S.W., Scherrmann, J.M. and Baud, F.J. (1996). Markedly altered colchicine kinetics in a fatal intoxication: examination of contributing factors. Hum. Exp. Toxicol. *15,* 885–890.

Brncić, N., Visković, I., Perić, R., Dirlić, a., Vitezić, D. and Cuculić, D. (2001). Accidental plant poisoning with Colchicum autumnale: report of two cases. Croat. Med. J. *42,* 673–675.

Brvar, M., Kozelj, G., Mozina, M. and Bunc, M. (2004). Acute poisoning with autumn crocus (Colchicum autumnale L.). Wiener Klinische Wochenschrift *116,* 205 – 208.

CCP4 (1994). The CCP4 suite: programs for protein crystallography. Acta Crystallogr. D *50,* 760–763.

Cerquaglia, C., Diaco, M., Nucera, G., La Regina, M., Montalto, M. and Manna, R. (2005). Pharmacological and clinical basis of treatment of Familial Mediterranean Fever (FMF) with colchicine or analogues: an update. Curr. Drug Targets Inflamm. Allergy *4,* 117–124.

Chen, V.B., Arendall, W.B., 3rd, Headd, J.J., Keedy, D.A., Immormino, R.M., Kapral, G.J., Murray, L.W., Richardson, J.S. and Richardson, D.C. (2010). MolProbity: all-atom structure validation for macromolecular crystallography. Acta Crystallogr. D *66,* 12–21.

Colovos, C. and Yeates, T.O. (1993). Verification of protein structures: patterns of nonbonded atomic interactions. Protein Sci. *2*, 1511–1519.

Correnti, C. and Strong, R.K. (2012). Mammalian siderophores, siderophore-binding lipocalins, and the labile iron pool. J. Biol. Chem. *287*, 13524–13531.

Danel, V.C., Wiart, J.F., Hardy, G.a., Vincent, F.H. and Houdret, N.M. (2001). Self-poisoning with Colchicum autumnale L. flowers. J. Toxicol. Clin. Toxicol. *39*, 409–411.

Dauner, M., Eichinger, A., Lücking, G., Scherer, S. and Skerra, A. (2018). Reprogramming human siderocalin to neutralize petrobactin, the essential iron scavenger of anthrax bacillus. Angew. Chem. Int. Ed. Engl. *57*, 14619-14623.

DeLano, W.L. (2002) The PyMOL Molecular Graphics System. San Carlos, CA; USA, DeLano Scientific.

Deveaux, M., Hubert, N. and Demarly, C. (2004). Colchicine poisoning: case report of two suicides. Forensic Sci. Int. *143*, 219–222.

Eddleston, M., Fabresse, N., Thompson, A., Al Abdulla, I., Gregson, R., King, T., Astier, A., Baud, F.J., Clutton, R.E. and Alvarez, J.-C. (2018). Anti-colchicine Fab fragments prevent lethal colchicine toxicity in a porcine model: a pharmacokinetic and clinical study. Clin. Toxicol., 1-9.

Emsley, P. and Cowtan, K. (2004). Coot: model-building tools for molecular graphics. Acta Crystallogr. D *60*, 2126–2132.

Eyer, F., Steimer, W., Nitzsche, T., Jung, N., Neuberger, H., Müller, C., Schlapschy, M., Zilker, T. and Skerra, A. (2012). Intravenous application of an anticalin dramatically lowers plasma digoxin levels and reduces its toxic effects in rats. Toxicol. Appl. Pharmacol. *263*, 352–359.

Fabresse, N., Allard, J., Sardaby, M., Thompson, A., Clutton, R.E., Eddleston, M. and Alvarez, J.-C. (2017). LC–MS/MS quantification of free and Fab-bound colchicine in plasma, urine and organs following colchicine administration and colchicine-specific Fab fragments treatment in Göttingen minipigs. Journal of Chromatography B *1060*, 400-406.

Folpini, a. and Furfori, P. (1995). Colchicine toxicity – clinical features and treatment. Massive overdose case report. J. Toxicol. Clin. Toxicol. *33*, 71–77.

Friedrich, L., Kornberger, P., Mendler, C.T., Multhoff, G., Schwaiger, M. and Skerra, A. (2017). Selection of an Anticalin® against the membrane form of Hsp70 via bacterial surface display and its theranostic application in tumour models. Biol. Chem., in press. DOI: 10.1515/hsz-2017-0207.

Ganfornina, M.D., Gutierrez, G., Bastiani, M. and Sanchez, D. (2000). A phylogenetic analysis of the lipocalin protein family. Mol. Biol. Evol. *17*, 114-126.

Gebauer, M., Schiefner, A., Matschiner, G. and Skerra, A. (2013). Combinatorial design of an Anticalin directed against the extra-domain B for the specific targeting of oncofetal fibronectin. J. Mol. Biol. *425*, 780–802.

Gebauer, M. and Skerra, A. (2012). Anticalins: Small engineered binding proteins based on the lipocalin scaffold. Methods Enzymol. *503*, 157–188.

Goetz, D.H., Holmes, M.A., Borregaard, N., Bluhm, M.E., Raymond, K.N. and Strong, R.K. (2002). The neutrophil lipocalin NGAL is a bacteriostatic agent that interferes with siderophore-mediated iron acquisition. Mol. Cell *10*, 1033–1043.

Hartung, E.F. (1954). History of the use of Colchicum and related medicaments in gout. Ann. Rheum. Dis. *13*, 190–200.

Hooft, R.W., Vriend, G., Sander, C. and Abola, E.E. (1996). Errors in protein structures. Nature *381*, 272.

Joosten, R.P., Long, F., Murshudov, G.N. and Perrakis, A. (2014). The PDB_REDO server for macromolecular structure model optimization. IUCrJ *1*, 213–220.

Jose, J., Krämer, J., Klauser, T., Pohlner, J. and Meyer, T.F. (1996). Absence of periplasmic DsbA oxidoreductase facilitates export of cysteine-containing passenger proteins to the Escherichia coli cell surface via the Igaβ autotransporter pathway. Gene *178*, 107-110.

Kabsch, W. and Sander, C. (1983). Dictionary of protein secondary structure: pattern recognition of hydrogen-bonded and geometrical features. Biopolymers *22*, 2577–2637.

Kim, H.J., Eichinger, A. and Skerra, A. (2009). High-affinity recognition of lanthanide(III) chelate complexes by a reprogrammed human lipocalin 2. J. Am. Chem. Soc. *131*, 3565–3576.

Klintschar, M., Beham-Schmidt, C., Radner, H., Henning, G. and Roll, P. (1999). Colchicine poisoning by accidental ingestion of meadow saffron (Colchicum autumnale): pathological and medicolegal aspects. Forensic Sci. Int. *106*, 191–200.

Kreutzberg, G.W. (1969). Neuronal dynamics and axonal flow, IV. Blockage of intra-axonal transport by colchicine. Proc. Natl. Acad. Sci. USA *62*, 722–728.

Krissinel, E. and Henrick, K. (2007). Inference of macromolecular assemblies from crystalline state. J. Mol. Biol. *372*, 774–797.

Laskowski, R.A., MacArthur, M.W., Mos, D.S. and Thornton, J.M. (1993). PROCHECK: a program to check the stereochemical quality of protein structures. J. Appl. Crystallogr. *26*, 283–291.

Link, L.H., Bindels, A.J.G.H., Brassé, B.P., Intven, F.A., Grouls, R.J.E. and Roos, A.N. (2014). Severe colchicine intoxication; always lethal ?!? Neth. J. Crit. Care, 19–21.

Luthy, R., Bowie, J.U. and Eisenberg, D. (1992). Assessment of protein models with three-dimensional profiles. Nature *356*, 83–85.

Malakhov, M.P., Mattern, M.R., Malakhova, O.a., Drinker, M., Weeks, S.D. and Butt, T.R. (2004). SUMO fusions and SUMO-specific protease for efficient expression and purification of proteins. J. Struct. Funct. Genomics *5*, 75-86.

Malawista, S.E. (1968). Colchicine: A common mechanism for its anti-inflammatory and anti-mitotic effects. Arthritis Rheum. *11*, 191–197.

McCreery, T. (1997). Digoxigenin labeling. Mol. Biotechnol. *7*, 121-124.

Miyachi, Y., Taniguchi, S., Ozaki, M. and Horio, T. (1981). Colchicine in the treatment of the cutaneous manifestations of Behcet's disease. Br. J. Dermatol. *104*, 67–70.

Nagesh, K.R., Menezes, R.G., Rastogi, P., Naik, N.R., Rasquinha, J.M., Senthilkumaran, S. and Fazil, A. (2011). Suicidal plant poisoning with Colchicum autumnale. J. Forensic Leg. Med. *18*, 285–287.

Niel, E. and Scherrmann, J.-M. (2006). Colchicine today. Joint Bone Spine *73*, 672–678.

Nuki, G. (2008). Colchicine: Its mechanism of action and efficacy in crystal-induced inflammation. Curr. Rheumatol. Rep. *10*, 218–227.

Panda, D., Daijo, J.E., Jordan, M.a. and Wilson, L. (1995). Kinetic stabilization of microtubule dynamics at steady state in vitro by substoichiometric concentrations of tubulin-colchicine complex. Biochemistry *34*, 9921–9929.

Peake, P.W., Pianta, T.J., Succar, L., Fernando, M., Buckley, N.a. and Endre, Z.H. (2015). Fab fragments of ovine antibody to colchicine enhance its clearance in the rat. Clin. Toxicol., 1-6.

Pontius, J., Richelle, J. and Wodak, S.J. (1996). Deviations from standard atomic volumes as a quality measure for protein crystal structures. J. Mol. Biol. *264*, 121–136.

Rauth, S., Hinz, D., Borger, M., Uhrig, M., Mayhaus, M., Riemenschneider, M. and Skerra, A. (2016). High-affinity Anticalins with aggregation-blocking activity directed against the Alzheimer beta-amyloid peptide. Biochem. J. *473*, 1563–1578.

Richter, a., Eggenstein, E. and Skerra, a. (2014). Anticalins: Exploiting a non-Ig scaffold with hypervariable loops for the engineering of binding proteins. FEBS Lett. *588*, 213-218.

Rochdi, M., Sabouraud, a., Girre, C., Venet, R. and Scherrmann, J.M. (1994). Pharmacokinetics and absolute bioavailability of colchicine after i.v. and oral administration in healthy human volunteers and elderly subjects. Eur. J. Clin. Pharmacol. *46*, 351–354.

Rothe, C. and Skerra, A. (2018). Anticalin® proteins as therapeutic agents in human diseases. Biodrugs *32*, 233–243.

Sabouraud, A., Urtizberea, M., Grandgeorge, M., Gattel, P., Makula, M.E. and Scherrmann, J.M. (1991). Dose-dependent reversal of acute murine colchicine poisoning by goat colchicine-specific Fab fragments. Toxicology *68*, 121–132.

Schiefner, A. and Skerra, A. (2015). The menagerie of human lipocalins: a natural protein scaffold for molecular recognition of physiological compounds. Acc. Chem. Res. *48*, 976–985.

Schlehuber, S., Beste, G. and Skerra, A. (2000). A novel type of receptor protein, based on the lipocalin scaffold, with specificity for digoxigenin. J. Mol. Biol. *297*, 1105-1120.

Schlehuber, S. and Skerra, A. (2005). Lipocalins in drug discovery: from natural ligand-binding proteins to "Anticalins". Drug Discov. Today *10*, 23-33.

Schmidt, T.G.M. and Skerra, A. (2007). The Strep-tag system for one-step purification and high-affinity detection or capturing of proteins. Nat. Protoc. *2*, 1528–1535.

Schönfeld, D., Matschiner, G., Chatwell, L., Trentmann, S., Gille, H., Hülsmeyer, M., Brown, N., Kaye, P.M., Schlehuber, S., Hohlbaum, A.M., *et al.* (2009). An engineered lipocalin specific for CTLA-4 reveals a combining site with structural and conformational features similar to antibodies. Proc. Natl. Acad. Sci. USA *106*, 8198–8203.

Skerra, A. (2000). Lipocalins as a scaffold. Biochim. Biophys. Acta *1482*, 337-350.

Stapczynski, J.S., Rothstein, R.J., Gaye, W.a. and Niemann, J.T. (1981). Colchicine overdose: report of two cases and review of the literature. Ann. Emerg. Med. *10*, 364–369.

Terrien, N., Urtizberea, M. and Scherrmann, J.M. (1990). Reversal of advanced colchicine toxicity in mice with goat colchicine-specific antibodies. Toxicol. Appl. Pharmacol. *104*, 504-510.

Vogt, M. and Skerra, A. (2001). Bacterially produced apolipoprotein D binds progesterone and arachidonic acid, but not bilirubin or E-3M2H. J. Mol. Recognit. *14*, 79-86.

Voss, E.W. (1984) *Fluorescein hapten: An immunological probe*. CRC Press, Boca Raton, FL.

Wallace, L. and Ertel, H. (1970). Colchicine plasma levels: implications as to pharmacology and mechanism of action. Am. J. Med. *48***,** 443–448.

Walsh, G. (2007) *Pharmaceutical biotechnology: Concepts and applications*. Wiley.

Wehner, F., Musshoff, F., Schulz, M., Martin, D. and Wehner, H.-D. (2006). Detection of colchicine by means of LC-MS/MS after mistaking meadow saffron for bear's garlic. Forensic Sci. Med. Pathol. *2***,** 193–197.

Weichenberger, C.X. and Sippl, M.J. (2007). NQ-Flipper: recognition and correction of erroneous asparagine and glutamine side-chain rotamers in protein structures. Nucleic Acids Res. *35***,** W403-W406.

Wilchek, M., Bayer, E.A. and Livnah, O. (2006). Essentials of biorecognition: The (strept) avidin–biotin system as a model for protein–protein and protein–ligand interaction. Immunol. Lett. *103***,** 27-32.

Tables and figures

Table 1 Dissociation constants of colchicine-specific lipocalin variants from fluorescence titration.

Variant	K_D ± SD (nm)
D6.1	3.6 ± 0.1
D6.1(V69M)	0.26 ± 0.03
D6.1(I80T)	2.6 ± 0.1
D6.1(F83L)	1.3 ± 0.1
D6.1(V69M/I80T)	0.23 ± 0.01
D6.1(V69M/F83L)	0.094 ± 0.025
D6.1(I80T/F83L)	0.60 ± 0.07
D6.1(V69M/I80T/F83L) = D6.2	0.047 ± 0.004

Titration was performed with 100 nM protein. SD is standard deviation of the curve fitting.

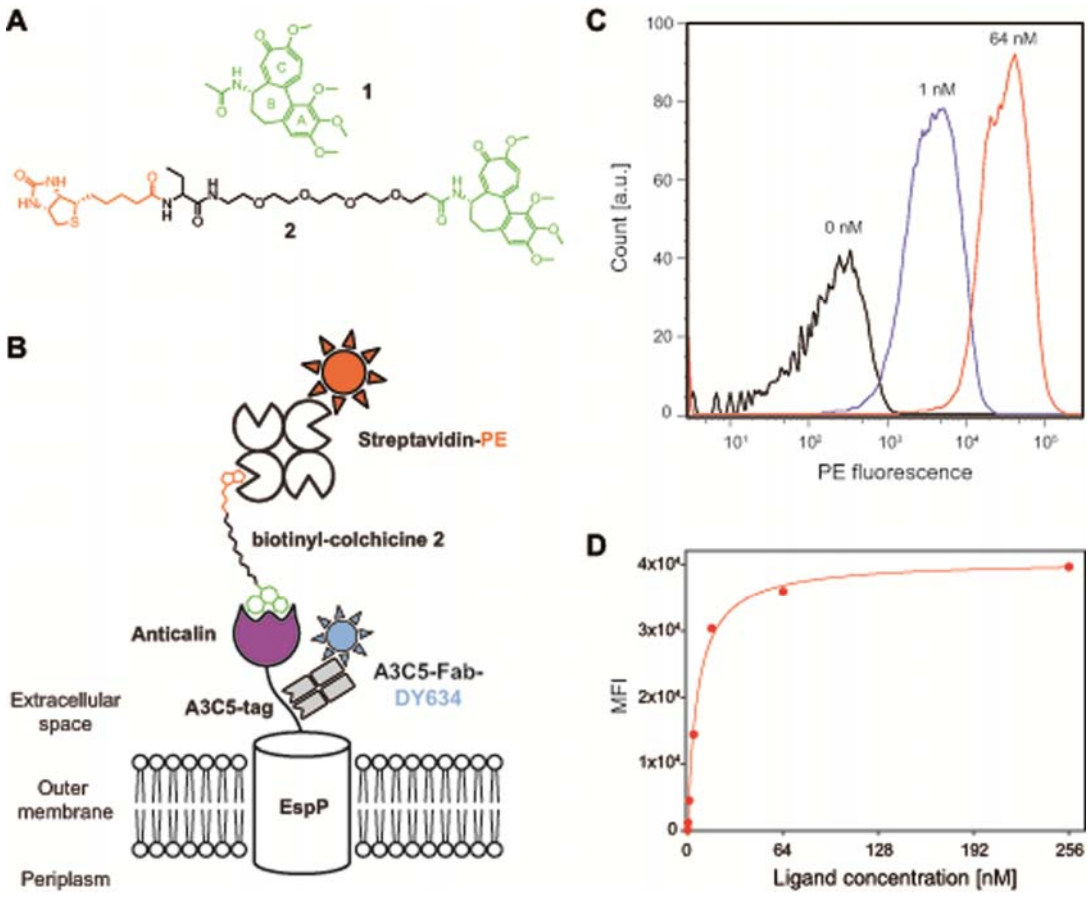

Figure 1 Overview of the selection process for lipocalins with novel ligand specificity as applied in this study**.**

(A) Colchicine (**1**) and biotinyl-colchicine with a PEG_3-Abu linker (**2**) served for selection of cognate lipocalin variants via phagemid display and bacterial surface display. (B) Scheme of *E. coli* surface display. Mediated by a signal peptide, the lipocalin initially gets secreted into the bacterial periplasm as a fusion protein with the β-domain of the autotransporter EspP, which enables its insertion into the outer bacterial membrane, followed by translocation onto the extracellular side. A Fab fragment recognizing the A3C5-tag labeled with the fluorescent dye DY634 was used for quantification of the number of lipocalin proteins displayed per bacterial cell. Bound biotinyl-colchicine (**2**) was separately probed with streptavidin-phycoerythrin (PE) conjugate. (C) Exemplary FACS histograms (for biotinyl-colchicine at the indicated concentration, detected with streptavidin-PE) during on-cell affinity determination for the cultured clone D6.1. (D) FACS affinity titration of the clone D6.1. The curve was obtained by applying a dilution series of biotinyl-colchicine ($[L]_{tot}$) to the bacterial cells, followed by FACS analysis as shown in panel (C). Mean fluorescence intensities (MFI) were fitted to a hyperbolic equation to yield the dissociation constant (K_D): $MFI = MFI_{max} \times L_{tot} / (K_D + L_{tot})$.

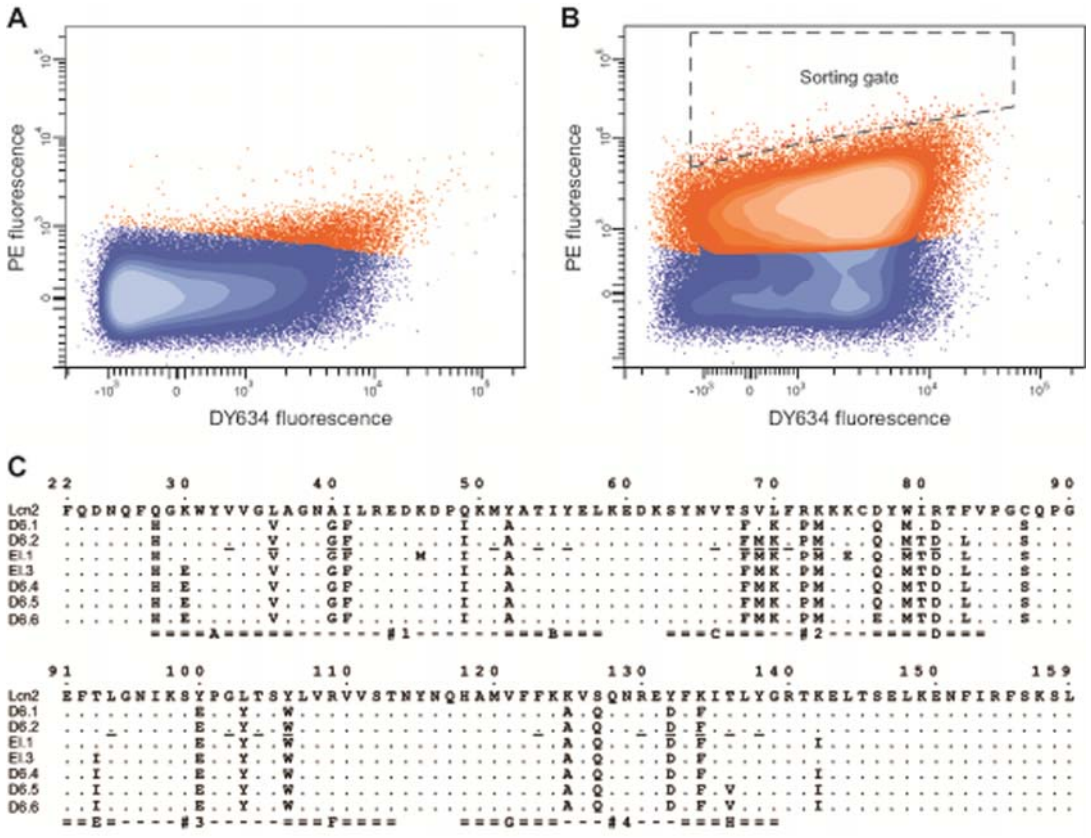

Figure 2 Affinity maturation of colchicine-specific lipocalin variants.

(A) Two-dimensional FACS signal of the original clone D6.1 (cf. Figure 1) and (B) of the error-prone library prepared from this variant after the sixth (last) FACS cycle. Both FACS measurements were made after incubation with 10 nM biotinyl-colchicine (**2**) for 1 min, followed by overnight incubation with 10 μM free colchicine (competition step). The DY634 signal (x-axis) represents the level of lipocalin expression on the bacterial cell surface whereas the PE signal (y-axis) indicates binding of the biotinylated ligand. Bacterial counts giving rise to relevant binding signals (exceeding those of wild-type Lcn2) are colored orange. The selection step illustrated in (B) led to the identification of in total 20 variants; three predominant mutations from these were combined to generate the version D6.2. (C) Amino acid sequence alignment of the lipocalin variants selected in the course of this study. The top line represents human wild-type Lcn2. β-Strands A to H of the lipocalin and flexible loops #1 to #4 are indicated. Variants EI.1 and EI.3 were obtained by affinity maturation of D6.2, variants D6.4 to D6.6 were constructed by rational mutagenesis. Residues of D6.2 that form van der Waals contacts with colchicine, as revealed by the crystal structure (see Table S2), are underlined.

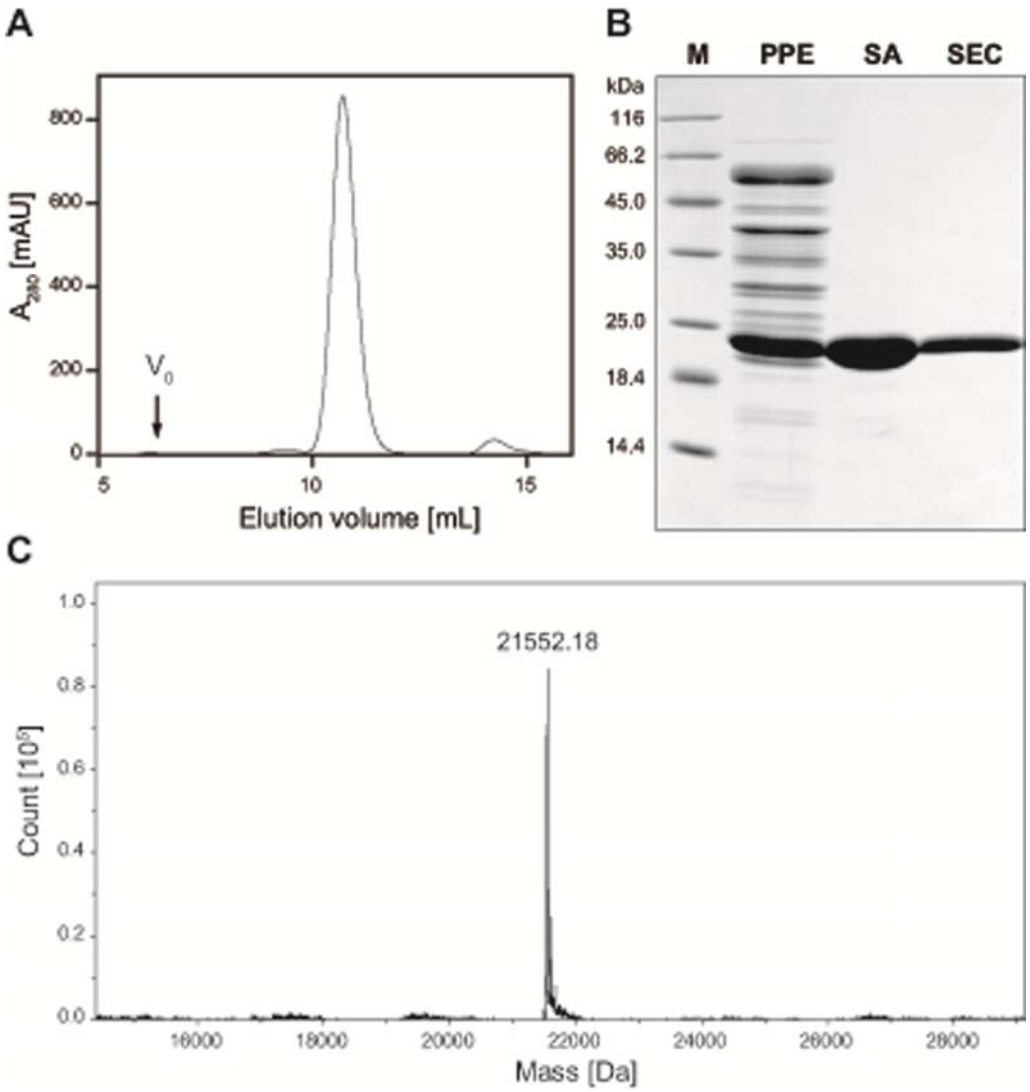

Figure 3 Biochemical characterization of the Colchicalin D6.2.

(A) Size-exclusion chromatography (SEC) of D6.2 on a Superdex S75 10/300 column (bed volume V_t = 24 ml) with PBS as running buffer. The elution volume of 10.7 ml corresponds to a molecular mass of ~22 kDa. (B) SDS-PAGE illustrating purification of D6.2: PPE, periplasmic extract; SA, eluate from *Strep*-Tactin affinity chromatography; SEC, eluate from size-exclusion chromatography; M, molecular size marker. (C) ESI-TOF mass-spectrum of purified D6.2, essentially matching the theoretical mass of 21 551.52 Da that was calculated from the protein sequence (including loss of 2 Da due to oxidative formation of the structural disulfide bond inherent to the Lcn2 scaffold).

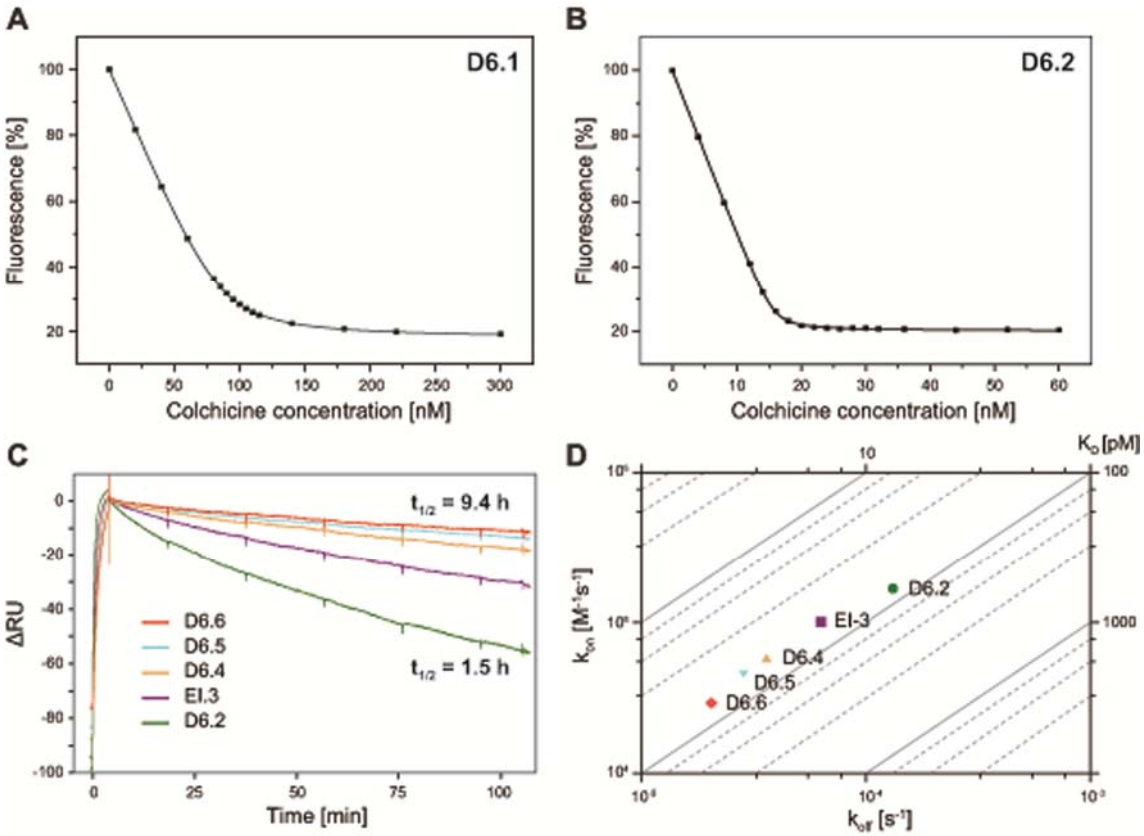

Figure 4 Affinity determination for the lipocalin variants selected against colchicine. Determination of equilibrium binding constants for the initially selected variant D6.1 and its improved version D6.2 by fluorescence titration with colchicine in PBS. The change in fluorescence at 345 nm (upon excitation at 280 nm) was monitored when adding 0.25–2 µl aliquots of ligand solution in the same buffer, and the fluorescence intensity was normalized to a 100% starting value. (A) D6.1 was titrated at 100 nM, leading to a K_D value of 3.6 ± 0.1 nM (error is the standard deviation of curve fitting). (B) D6.2 was titrated at a lower protein concentration of 20 nM in triplicate in order to improve resolution of the data around the point of equimolarity, leading to a K_D value of 120 ± 26 pM (error is the standard deviation of the triplicate titration; the depicted titration curve revealed K_D = 111 pM). (C) Measurement of kinetic binding constants via real-time surface plasmon resonance (SPR) spectroscopy. The complex half-life increased from 1.5 h for D6.2 to 9.4 h for D6.6. (D) k_{on}/k_{off} plot of the kinetic constants determined by SPR. The diagonal lines mark ratios corresponding to equal dissociation constants (K_D). Interestingly, slower dissociation rate coincided with a lower association rate for all lipocalin variants from the later stage of optimization, resulting in almost unchanged ligand affinity.

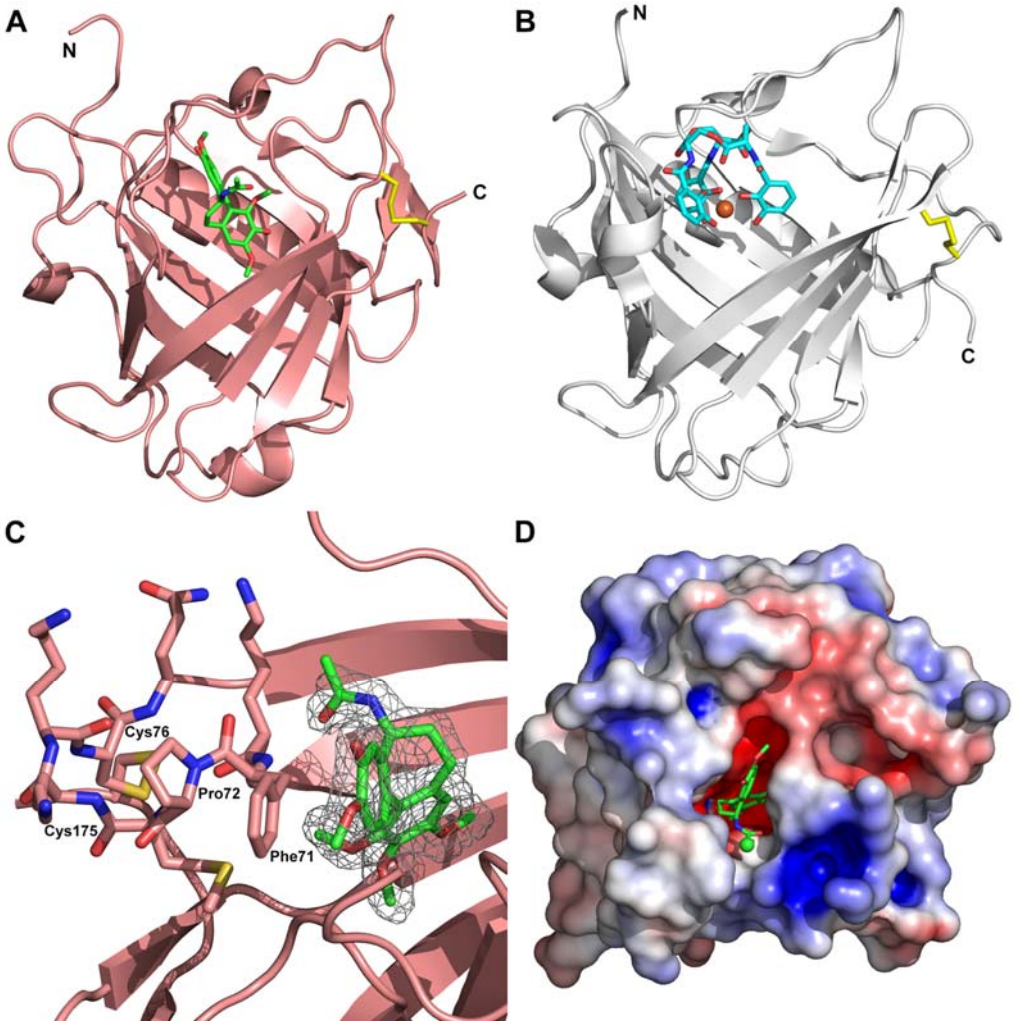

Figure 5 X-ray crystallographic analysis of the Colchicalin•colchicine complex. (A) The Colchicalin Δ4-D6.2(M69Q) in complex with colchicine (**1**). The protein is shown in ribbon representation colored salmon, the carbon atoms of colchicine are colored green. The C-terminal disulfide bridge connecting Cys76 and Cys175 is depicted as sticks in yellow. (B) Similar view of the Lcn2 crystal structure (K125A mutant) in complex with ferric enterobactin (PDB ID: 3CMP). The protein is colored light gray, the carbon atoms of enterobactin are colored cyan and the central iron ion is shown as dark red sphere. (C) Close-up view on the bound colchicine from (A) and its $2F_O$-F_C electron density contoured at 1 σ. Relevant residues in loop #2 (Lys70–Gln77) of Colchicalin, which harbors Pro72 in *cis*-configuration as well as Cys76 that participates in the disulfide bridge, are shown as sticks. (D) Electrostatic surface representation of Colchicalin with negatively charged areas colored red (-5 k_BT/e) and positively charged areas colored blue (5 k_BT/e). The C-atom of the acetyl group attached to the primary amino function of the bound colchicine, which served to connect the PEG linker in the biotin and amino conjugates (**2** and **8**), is highlighted as sphere.

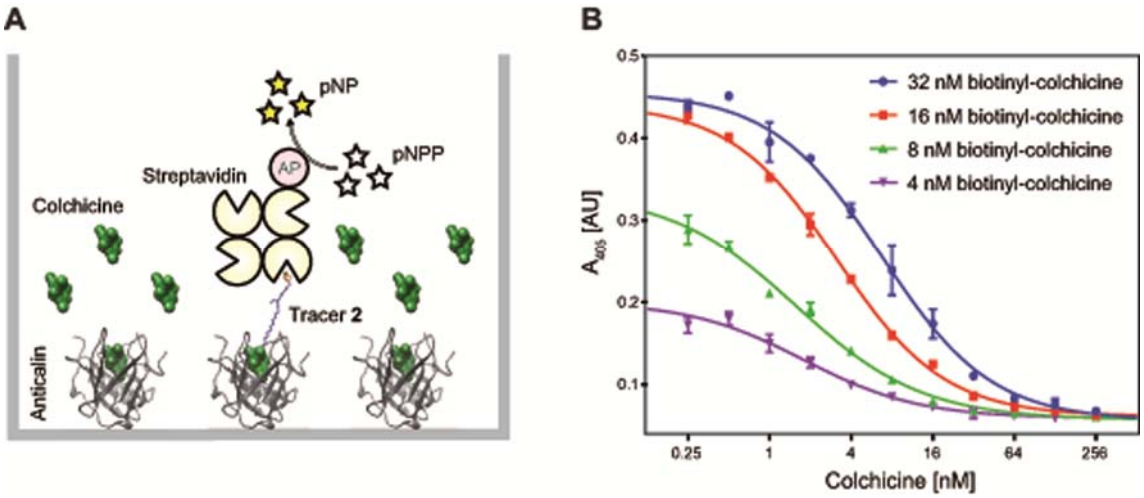

Figure 6 Development of a competitive ELISA based on the Colchicalin D6.2 for the quantification of colchicine.

(A) Schematic setup of the competitive ELISA. The bottom of a microtiter plate is coated with D6.2, then a sample with varying colchicine concentration spiked with tracer (biotinyl-colchicine, **2**) is added and, after washing, bound tracer is detected by means of a streptavidin-alkaline phosphatase (AP) conjugate. (B) Exemplary readout of the ELISA for colchicine at varying concentration in PBS using different concentrations of the biotinyl-colchicine tracer. End-point absorbance at 405 nm was measured after 30 min signal development with the substrate *p*-nitrophenylphosphate. Data points were acquired in duplicates; the error bars represent standard deviations for n = 2. The data were fitted to the equation: $A_{405} = A_{max} + (A_{min} - A_{max}) / (1 + \left(\frac{[colchicine]}{EC_{50}}\right)^{slope})$.

Supplementary Material

Table S1 Crystallographic analysis and refinement statistics.

	Colchicalin•colchicine
Crystal Data:	
Space group	$P4_122$
Unit cell dimensions a, b, c [Å], $\alpha=\beta=\gamma=90°$	46.68, 46.68, 136.85
molecules per asym. unit	1
Data Collection:	
Wavelength [Å]	0.89429
Resolution range [Å][a]	46.68–2.20 (2.32–2.20)
$I/\sigma[I]$[a]	6.3 (1.9)
R_{merge} [%][a, b]	9.4 (41.0)
Unique reflections	8323
Multiplicity[a]	10.3 (9.0)
Completeness[a]	99.9 (99.4)
Refinement:	
R_{cryst} / R_{free}[c]	19.7/26.6
Protein atoms	1394
Ligand atoms	29
Solvent atoms	36
Average B-factor protein [Å^2]	
Protein	36.9
Ligand	25.3
Water	28.1
Geometry:	
R.m.s.d. bond lengths, angles [Å, °]	0.011, 1.634
Ramachandran analysis[d]: core, allowed, generously allowed, disallowed [%]	91.2, 8.1, 0.0, 0.7

[a] Values in parentheses are for the highest resolution shell.

[b] $R^{merge} = \sum_h \sum_i |I(h) - \langle I(h) \rangle| / \sum_h \sum_i I(h)$ $\quad R_{cryst} = \sum_h ||F_o(h)| - |F_c(h)|| / \sum_h |F_o(h)|$

[c] R^{free} is R^{cryst} with 5 % of the reflections that were randomly selected and excluded from refinement (Brunger, 1997).

[d] calculated with PROCHECK

Table S2 Residues of the Colchicalin•colchicine complex that form van der Waals contacts with the ligand. Buried surfaces are given for each of the contacting amino acids. The total buried surface comprises 547.8 Å^2, the total ligand surface comprises 617.7 Å^2.

Residue	Buried surface [Å^2]	Residue	Buried surface [Å^2]	Residue	Buried surface [Å^2]
Val33	6.4	Gln69	6.0	Trp106	37.2
Val36	3.7	Lys70	13.0	Phe123	10.2
Gly40	8.3	Phe71	64.7	Arg130	12.8
Phe41	17.7	Met73	2.6	Asp132	12.5
Met51	12.6	Met79	13.8	Phe134	34.9
Thr54	2.6	Asp81	3.0	Thr136	6.2
Tyr56	1.4	Leu94	15.6	Tyr138	8.6
Val66	5.5	Gly102	1.8		
Phe68	45.0	Thr104	0.3		

Table S3 Kinetic constants for colchicine binding by Colchicalins determined via real-time SPR.

Mutant	k_{on} [M^{-1}s^{-1}]	SE	k_{off} [s^{-1}]	SE	K_D [pM]	$t_{1/2}$ [h]
D6.2	1.67 x10^5	830	1.32 x10^{-4}	1.01 x10^{-7}	790	1.5
EI.1	7.44 x10^4	54	6.17 x10^{-5}	8.89 x10^{-8}	829	3.1
EI.3	1.03 x10^5	204	5.64 x10^{-5}	2.71 x10^{-7}	548	3.4
EI.3(K142I) = D6.4	5.8 x10^4	71	3.61 x10^{-5}	3.89 x10^{-8}	622	5.3
D6.4(Q77E)	6.41 x10^4	188	2.89 x10^{-5}	3.69 x10^{-8}	451	6.7
D6.4(T136V) = D6.5	4.60 x10^4	102	2.85 x10^{-5}	4.80 x10^{-8}	620	6.8
D6.5(Q77E) = D6.6	2.92 x10^4	36	2.05 x10^{-5}	2.73 x10^{-8}	702	9.4

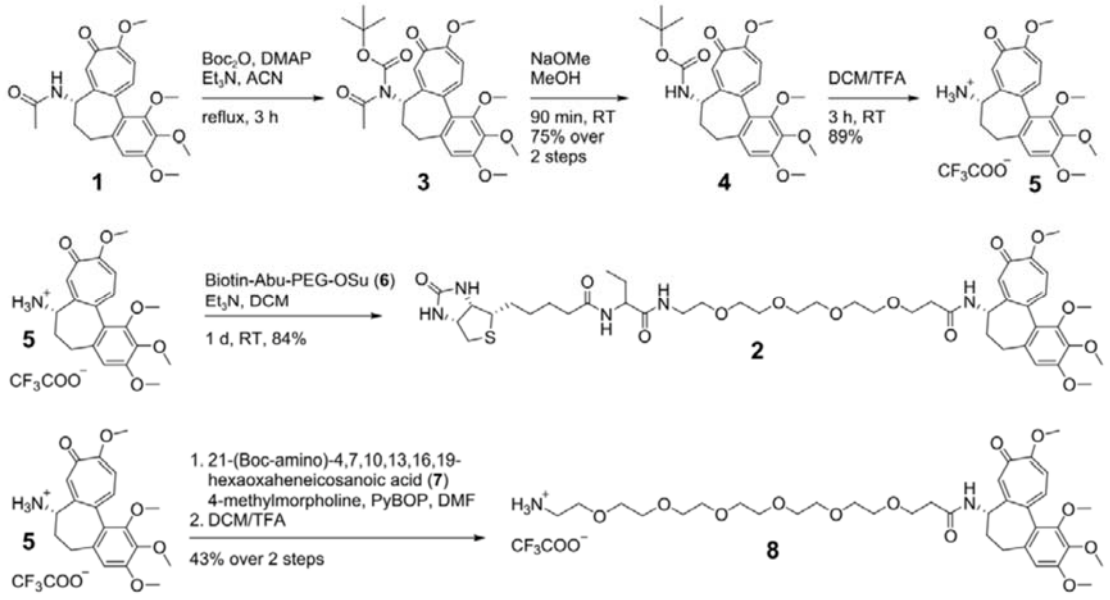

Figure S1 Chemical synthesis of colchicine derivatives carrying a biotin moiety or amino-PEG linker.

Deacetylation of colchicine (**1**) was performed via Boc protection of the amide nitrogen, deacetylation and Boc cleavage. A biotinylated derivative **2** was obtained after ligation of deacetylcholchicine (**5**) with Biotin-Abu-PEG_3-OSu (**6**). Coupling of deacetylcholchicine with a Boc-protected amino-PEG_5-carboxylic acid linker **7**, followed by Boc deprotection, led to the colchicine derivative **8** for immobilization on carboxy-functionalized SPR sensor chips.

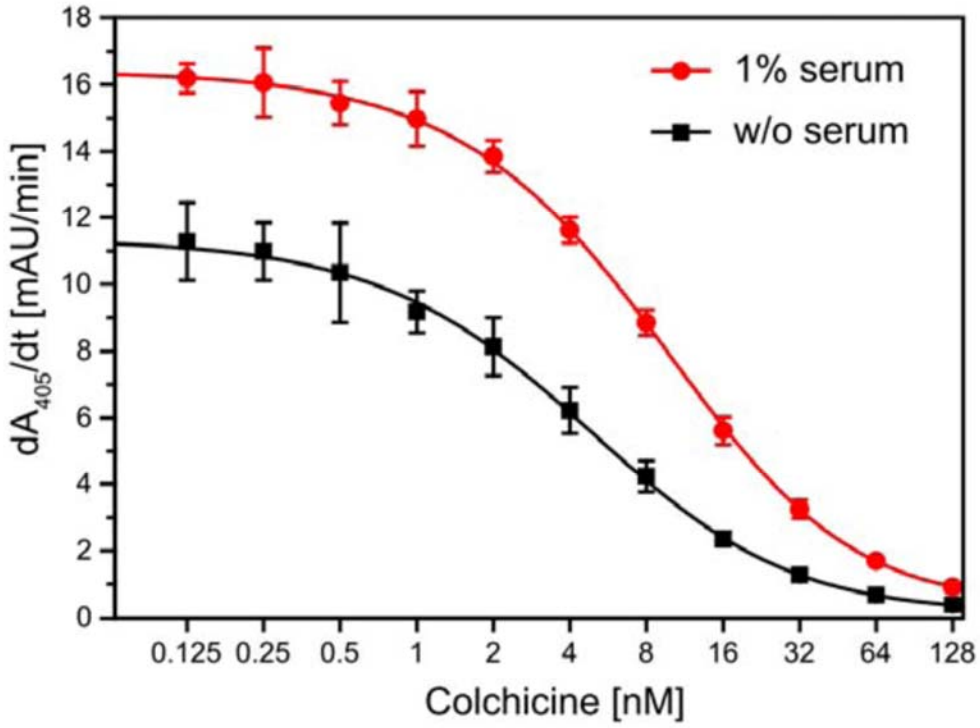

Figure S2 Competitive ELISA for the detection of free colchicine: effect of human serum in the sample.

The assay was performed as described in Figure 6 and in the Methods section. Increase of absorbance was measured for 30 min. One analyte sample was prepared as a dilution series in PBS, the other one in the presence of 1% v/v human serum. Biotinyl-colchicine **2** was added as tracer at 10 nM concentration to both samples. Data were collected in quadruplicates and fitted as in Figure 6; the error bars represent standard deviation.